

circRNA circARNT2 Suppressed the Sensitivity of Hepatocellular Carcinoma Cells to Cisplatin by Targeting the miR-155-5p/PDK1 Axis

Yueyong Li,¹ Yingjun Zhang,² Shuai Zhang,^{3,4} Deyou Huang,⁵ Baosheng Li,⁵ Gencheng Liang,¹ Yingning Wu,¹ Qiulan Jiang,¹ Longhua Li,¹ Cheng Lin,¹ Zhonghen Wei,¹ and Lingzhang Meng⁶

¹Department of Interventional Medicine, the Affiliated Hospital of Youjiang Medical University for Nationalities, Baise 533000, China; ²Department of Medical Imageology, Hunan University of Medicine, Huaihua 418000, China; ³Department of Interventional Radiology, the Affiliated Hospital of Guizhou Medical University, Guiyang 550000, China; ⁴Department of Interventional Radiology, the Affiliated Cancer Hospital of Guizhou Medical University, Guiyang 550000, China; ⁵Department of Radiology, the Affiliated Hospital of Youjiang Medical University for Nationalities, Baise 533000, China; ⁶Center for Systemic Inflammation Research, School of Preclinical Medicine, Youjiang Medical University for Nationalities, Baise City 533000, Guangxi Province, China

Circular RNA (circRNA) is a novel subclass of noncoding-RNA molecules that participate in development and progression of a variety of human diseases via sponging microRNAs (miRNAs). Until now, the contributions of circRNAs in chemoresistance of hepatocellular carcinoma (HCC) remain largely unknown. In the present study, we aimed to investigate the role of circRNA in cisplatin resistance of HCC. We investigated the expression of circRNAs in 5 paired cisplatin-sensitive and cisplatin-resistant HCC tissues by microarray analysis. The qRT-PCR analysis was to investigate the expression pattern of circARNT2 in HCC patient tissues and cell lines. Then, the effects of circARNT2 on cisplatin resistance, cell proliferation, and apoptosis were assessed in HCC *in vitro* and *in vivo*. circARNT2 was significantly upregulated in HCC tissues and cell lines. Overexpression of circARNT2 in HCC was significantly correlated with aggressive characteristics and served as an independent risk factor for overall survival in patients with HCC. *In vitro* experiments showed that knockdown of circARNT2 inhibited cell proliferation and enhances the cisplatin sensitivity of HCC cells. Furthermore, circARNT2 facilitates HCC progression *in vivo*. We demonstrated that circARNT2 acts as a sponge for miR-155-5p and verified that PDK1 is a novel target of miR-155-5p. In summary, our study demonstrated that circARNT2 modulates cisplatin resistance through miR-155-5p/PDK1 pathway. Our findings indicated that circARNT2 may serve as a promising therapeutic target for overcoming cisplatin resistance for HCC.

INTRODUCTION

Hepatocellular carcinoma (HCC) is the most common neoplasm of primary liver cancers, accounting for 85%–90% of all cases.¹ HCC is mainly associated with chronic liver disease and cirrhosis.² The treatment options for advanced-stage HCC are very limited. HCC can be treated with liver transplantation, surgical resection, radiofrequency ablation (RFA), transcatheter arterial chemoembolization

(TACE), and systemic chemotherapy.³ Because of late-stage detection and lack of effective therapies, the majority of patients lose the opportunity for surgery.⁴ Despite advances of modern treatments, chemotherapy is still a main and effective approach to control the development of HCC and prolong patients' life.⁵ However, many HCC cases show poor response to chemotherapy.^{6,7} Chemoresistance is still a major obstacle for HCC patients to obtain a satisfactory curative effect. Patients with advanced HCC have a poor prognosis. Thus, identifying new targets for therapeutic intervention and developing novel diagnostic approaches are in great need for early diagnosis and intervention for HCC.

Circular RNA (circRNA) is a novel type of noncoding RNA with a covalently closed loop, which is generated by the back-splicing of pre-mRNA.⁸ More newly identified circRNAs have been found using high-throughput sequencing and via further functional validation.⁹ Increasing evidences indicate that circRNAs are implicated in several pathophysiological processes including human cancers.^{10,11} Aberrant expression of circRNAs has been frequently observed in various cancers.^{12,13} Moreover, circRNAs regulate malignant behaviors of cancer cells, such as proliferation, apoptosis resistance, migration, invasion, and drug resistance.^{14,15} Although several circRNAs have been reported to participate in the tumorigenesis and progression of HCC,^{9,16,17} the expressions and roles of circRNA in chemoresistance of HCC remain unclear.

Received 28 January 2020; accepted 28 August 2020;
<https://doi.org/10.1016/j.omtn.2020.08.037>.

Correspondence: Zhonghen Wei, Department of Interventional Medicine, the Affiliated Hospital of Youjiang Medical University for Nationalities, Baise 533000, China.

E-mail: yougang1619@163.com

Correspondence: Lingzhang Meng, Center for Systemic Inflammation Research, School of Preclinical Medicine, Youjiang Medical University for Nationalities, Baise City, Guangxi Province, China.

E-mail: lingzhang.meng@ymcn.edu.cn

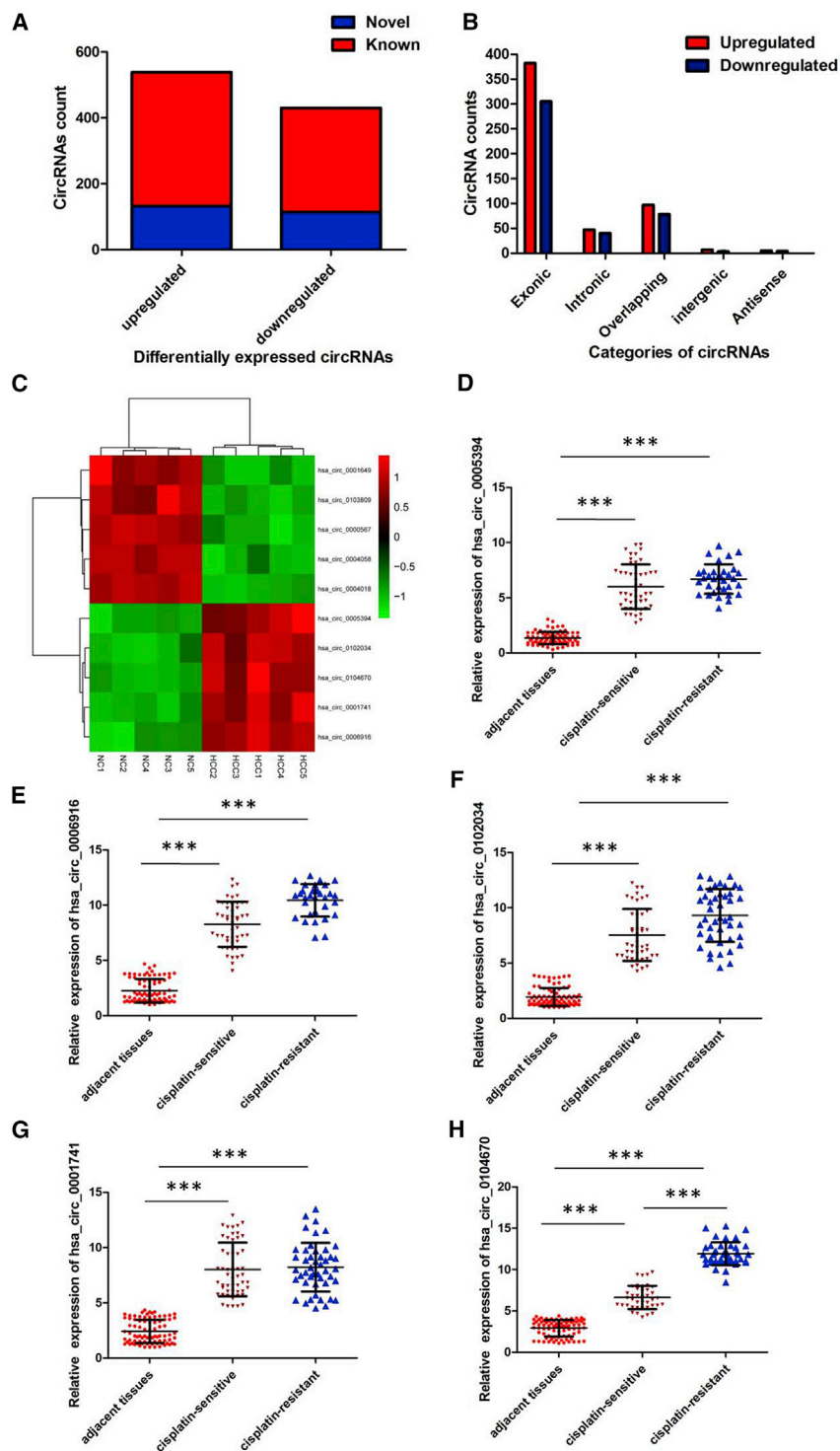


Figure 1. Upregulation of circARNT2 Is Associated with Cisplatin Resistance in HCC

(A) Among the 968 differentially expressed circRNAs, 246 were verified as novel circRNAs; 722 circRNAs were identified beforehand and listed in the circRNA database. (B) The number of upregulated (red) and downregulated (green) circRNAs according to their categories of formation mode. (C) The heatmap showed the top five most upregulated circRNAs and five most downregulated circRNAs between cisplatin-resistant HCC tissues and cisplatin-sensitive HCC tissues. (D) The level of hsa_circ_0005394 was significantly increased in cisplatin-resistant HCC tissues compared with the cisplatin-sensitive tissues. (E) The level of hsa_circ_0006916 was significantly increased in cisplatin-resistant HCC tissues compared with the cisplatin-sensitive tissues. (F) The level of hsa_circ_0102034 was significantly increased in cisplatin-resistant HCC tissues compared with the cisplatin-sensitive tissues. (G) The level of hsa_circ_0001741 was significantly increased in cisplatin-resistant HCC tissues compared with the cisplatin-sensitive tissues. (H) The level of hsa_circ_0104670 was significantly increased in cisplatin-resistant HCC tissues compared with the cisplatin-sensitive tissues. All tests were at least performed three times. Data were expressed as mean ± SD. ***p < 0.001.

derived from ARNT2 gene, and thus we termed as circARNT2. We further tested circARNT2 in HCC samples by qRT-PCR and the results showed that the expression of circARNT2 was markedly elevated both in HCC tissues and exosomes from HCC plasma. Gain-of-function investigations showed that circARNT2 overexpression suppressed cancer cell growth *in vivo* and *in vitro*. Subsequent studies displayed that circARNT2 could sensitize HCC cells to cisplatin by targeting the miR-155-5p/PDK1 signaling axis. Our findings will provide new insights into the regulatory mechanisms of circARNT2 in tumor progression and cisplatin resistance of HCC.

RESULTS
Upregulation of circARNT2 Is Associated with Cisplatin Resistance in HCC

To investigate the role of circRNAs in cisplatin resistance of HCC, we performed circRNAs array to identify the differentially expressed circRNAs. A total of 9,857 circRNAs were detected in 5 pairs of cisplatin-resistant HCC tissues and cisplatin-sensitive HCC tissues by the circRNA microarray analysis. Among them, 968 circRNAs were

significantly aberrantly expressed (p < 0.05 and fold-change [FC] > 2.0) between cisplatin-resistant HCC tissues and cisplatin-sensitive HCC tissues. Of these circRNAs, 538 were significantly upregulated and 430 were significantly downregulated in cisplatin-resistant

significantly aberrantly expressed (p < 0.05 and fold-change [FC] > 2.0) between cisplatin-resistant HCC tissues and cisplatin-sensitive HCC tissues. Of these circRNAs, 538 were significantly upregulated and 430 were significantly downregulated in cisplatin-resistant

Table 1. Association of circARNT2 Expression with Clinicopathological Features of HCC Patients

Characteristics	circARNT2 -21590444500Low (n = 41)	Expression High (n = 41)	p
Age, y			
≥ 50	21	24	0.657
Gender			
Female	19	22	0.659
Serum AFP			
≥ 20	16	22	0.268
Tumor size			
≥ 5.0 cm	14	28	0.003
TNM stage			
III/IV	8	18	0.031
Distant metastasis			
Yes	6	16	0.023

HCC tissues compared with cisplatin-sensitive HCC tissues. Among the 968 differentially expressed circRNAs, 246, including 132 upregulated ones and 114 downregulated ones, were verified as novel circRNAs; 722 circRNAs, including 406 upregulated and 316 downregulated ones, had been identified beforehand and listed in the circRNA database (circBase; <http://www.circbase.org>; Figure 1A). The 968 identified circRNAs were divided into five different categories on the basis of the way they were produced. Exonic circRNAs consisting of the protein-encoding exons accounted for 70.97% (687/968), intronic circRNAs from intron lariats comprised 8.99% (87/968), sense overlapping circRNAs that originated from exon and other sequence circRNAs comprised 18.08% (1555/968), intergenic circRNAs composed of unannotated sequences of the gene and antisense circRNAs originating from antisense regions equally comprised 1.96% (19/968; Figure 1B). Hierarchical clustering was then performed to demonstrate the five most upregulated circRNAs (hsa_circ_0005394, hsa_circ_0001741, hsa_circ_0006916, hsa_circ_0102034, and hsa_circ_0104670) and five most downregulated circRNAs (hsa_circ_0000567, hsa_circ_0004058, hsa_circ_0001649, hsa_circ_0103809, and hsa_circ_0004018) expression patterns among the sets (Figure 1C).

The five most upregulated circRNAs were selected and validated by qRT-PCR using 82 HCC and paired non-tumorous tissue samples. As shown in Figure 1D–1H, qPCR results further confirmed that circ_0104670 was significantly increased in HCC tissues compared with adjacent tissues, and its expression was higher in cisplatin-resistant HCC tissues than in the cisplatin-sensitive tissues. By browsing the human reference genome (GRCh37/hg19), we identified that hsa_circ_0104670 (chr15: 80767350–80772264) is derived from ARNT2, with a spliced mature sequence length of 4,914 base pairs (bp), and thus we named it circARNT2. We verified its existence in many circRNA databases. According to the circBase database,

circARNT2 is detected in normal human frontal cortex (http://www.circbase.org/cgi-bin/singlerecord.cgi?id=hsa_circ_0104670).

To further investigate the role of circARNT2 in HCC, we analyzed the relationship between circARNT2 expression in HCC tissues and clinicopathological characteristics of HCC patients. Using the median expression level of circARNT2 as cutoff value, patients who expressed circARNT2 equal to or greater than the average level were assigned to the “circARNT2 high” group. As shown in Table 1, high expression of circARNT2 in HCC tissues was significantly correlated with tumor size ($p = 0.003$), distant metastasis ($p = 0.031$), and TNM stage ($p = 0.023$) but not related to gender, age, and differentiation. In addition, further Kaplan-Meier survival analyses revealed that the HCC patients with high circARNT2 level had shorter overall survival than the patients had low circARNT2 level ($p = 0.012$, Figure 2A). We also found that circARNT2 was significantly increased in cisplatin resistant HCC cell lines (Hep3B-R and Huh7-R) compared with the parental HCC cell lines ($p < 0.01$; Figure 2B). These results suggest that circARNT2 is closely associated with cisplatin resistance in HCC.

circARNT2 Regulates the Cisplatin Chemosensitivity of HCC *In Vitro*

To further validate the expression level of circARNT2 on cisplatin resistance, we constructed circARNT2 shRNA and circARNT2 overexpression vector and performed loss- and gain-of-function studies by knocking down or overexpressing circARNT2 in HCC cells. First, we knocked down the expression of both circARNT2 and ARNT2 mRNA. Hep3B-R and Huh7-R cells were transfected with three kinds of circARNT2 shRNA (respectively sh-circARNT2 #1, sh-circARNT2 #2, or sh-circARNT2#3) or GFP lentivirus (sh-CTL), and the sequence only in the linear transcript (si-ARNT2). As expected, shRNA directed against the backsplice sequence knocked down only the circular transcript and did not affect the expression of linear species, and small interfering RNA (siRNA) targeting the sequence in the linear transcript knocked down only the linear transcript and did not affect the expression of the circular transcript in Hep3B-R and Huh7-R cells (Figures S1A–S1F; $p < 0.01$). Due to the highest efficiency of interference, sh-circARNT2 #3 was chosen for the subsequent experiments. Meanwhile, we infected Hep3B and Huh7 cells with the circARNT2 overexpression adenovirus (circARNT2 OE) or control GFP adenovirus (circARNT2 CTL). The qRT-PCR assay indicated the relative abundance of circARNT2 in Hep3B and Huh7 cells infected with adenovirus (Figures S1G and S1H; $p < 0.01$). We found that inhibition of circARNT2 significantly inhibited cells proliferation (Figures 2C and 2D) and induced apoptosis (Figures 2E and 2F) in Hep3B-R and Huh7-R cells compared with negative control. In addition, circARNT2 downregulation sensitized Hep3B-R and Huh7-R cells to cisplatin (Figures 2G and 2H).

circARNT2 Knockdown Inhibited the Growth of HCC *In Vivo*

Furthermore, the tumor suppressive effects of circARNT2 downregulation were also confirmed *in vivo*. Hep3B-R cells stably infected with sh-circARNT2 or sh-CTL were subcutaneously injected into each

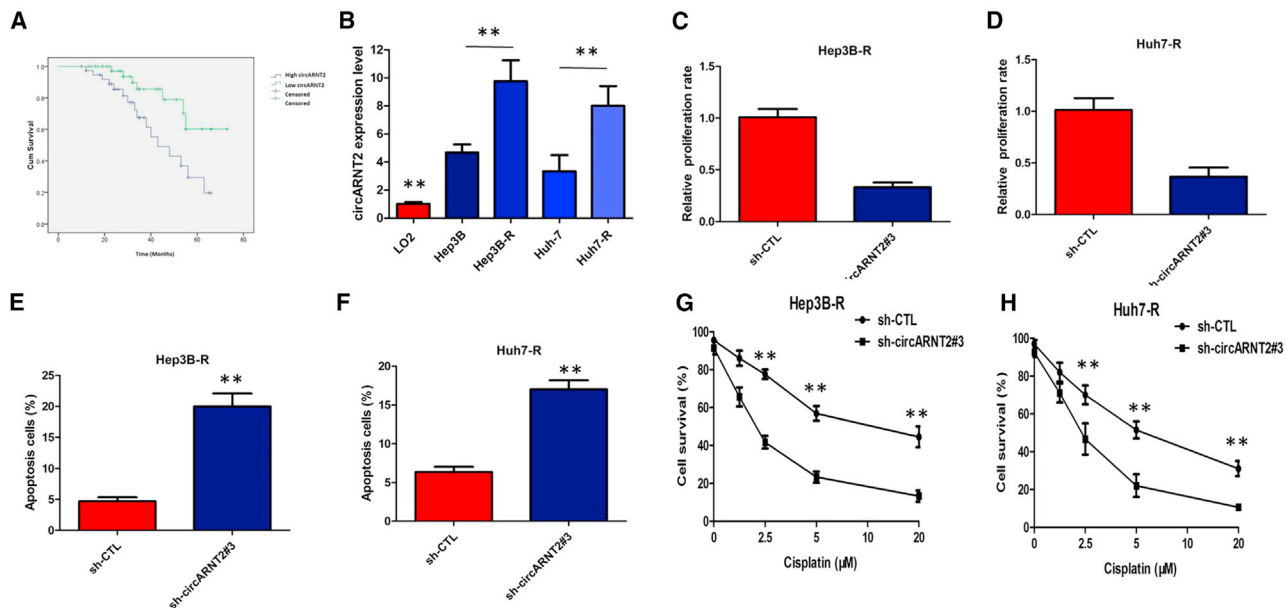


Figure 2. circARNT2 Regulates the Cisplatin Chemosensitivity of HCC *In Vitro*

(A) Kaplan-Meier survival analyses revealed that the HCC patients with high circARNT2 level had shorter overall survival than the patients had low circARNT2 level. (B) circARNT2 was significantly increased in cisplatin-resistant HCC cell lines (Hep3B-R and Huh7-R) compared with the parental HCC cell lines. (C) Inhibition of circARNT2 significantly inhibited cells proliferation of Hep3B-R cells. (D) Inhibition of circARNT2 significantly inhibited cells proliferation of Huh7-R cells. (E) Inhibition of circARNT2 significantly induced apoptosis of Hep3B-R cells. (F) Inhibition of circARNT2 significantly induced apoptosis of Huh7-R cells. (G) Inhibition of circARNT2 sensitized Hep3B-R cells to cisplatin. (H) Inhibition of circARNT2 sensitized Huh7-R cells to cisplatin. All tests were at least performed three times. Data were expressed as mean \pm SD. ** $p < 0.01$.

mouse. Our results showed that the tumor volumes in nude mice injected with sh-circARNT2-transfected Hep3B-R cells were smaller than in the control nude mice (Figure 3A). Tendencies in tumor weight were consistent with those in tumor volume (Figure 3B). The proliferative marker ki67 expression was decreased in tumor tissues of nude mice injected with sh-circARNT2-transfected Hep3B-R cells (Figure 3C).

Confirmation of the Circular Structure and Subcellular Localization of circARNT2

Next, we investigated the stability and localization of circARNT2 in HCC cells. Total RNAs from Hep3B-R and Huh7-R cells were isolated at the indicated time points after treatment with Actinomycin D, an inhibitor of transcription. Then qRT-PCR was performed to measure the level of circARNT2 and ARNT2 mRNA. The results showed that the half life of circARNT2 exceeded 24 h, whereas that of circARNT2 mRNA was about 4 h in both Hep3B-R and Huh7-R cells (Figures 4A and 4B). Furthermore, we found that circARNT2 was resistant to RNase R digestion (Figures 4C and 4D). These data confirmed that circARNT2 was a circular RNA. We then investigated the localization of circARNT2. The qRT-PCR of RNAs from nuclear and cytoplasmic fractions indicated that circARNT2 was predominantly localized in the cytoplasm of Hep3B-R and Huh7-R cells (Figures 4E and 4F). Collectively, the above data suggested that circARNT2 harbored a loop structure and was predominantly localized in the cytoplasm.

circARNT2 Functioned as a Molecular Sponge of miR-155-5p in HCC Cells

Given that many circRNAs can function as miRNA sponges in the cytoplasm, we determined whether circARNT2 may also bind to miRNAs as a sponge and regulate targets via the competitive endogenous RNA (ceRNA) mechanism. We therefore analyzed the sequence of circARNT2 using the miRanda algorithm and identified 199 miRNA-binding sites (Table S1); however, five miRNAs with relatively high scores (miRNA-155-5p, miRNA-1197, miRNA-155-5p, miRNA-1228, and miRNA-1236) were finally selected.

It is well known that miRNAs usually silence gene expression by combining with the Argonaute 2 (AGO2) protein and form the RNA-induced silencing complex (RISC). In the context of ceRNA mechanism, it might be a prevalent phenomenon that AGO2 could bind with both circRNAs and miRNAs. We therefore conducted an RNA immunoprecipitation (RIP) assay to pull down RNA transcripts that bind to AGO2 in Hep3B-R cells. Indeed, endogenous circARNT2 was efficiently pulled down by anti-Ago2 (Figure 5A). To further detect whether circARNT2 could sponge miRNAs, we performed a miRNA pull-down assay using biotin-coupled miRNA mimics (miRNA-155-5p, miRNA-1197, miRNA-155-5p, miRNA-1228, and miRNA-1236). Interestingly, circARNT2 was only efficiently enriched by miR-155-5p, but not by the other three miRNAs (Figure 5B). In order to further validate the interaction, circARNT2 sequence containing the putative or mutated miR-155-5p binding site was cloned into the downstream of luciferase reporter gene, generating wild-type

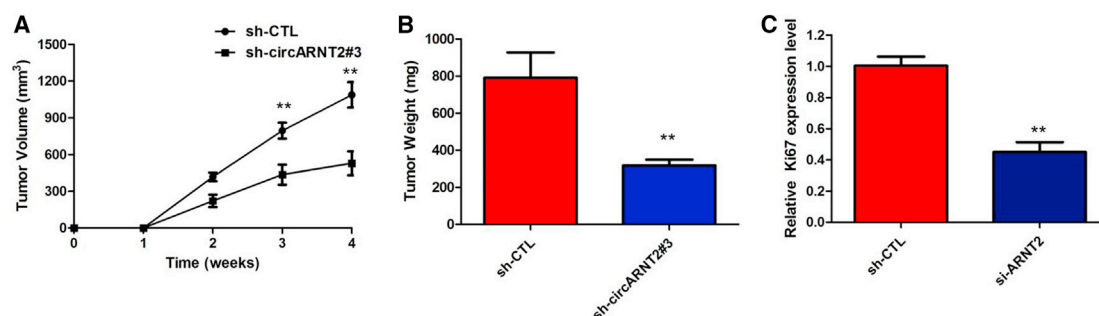


Figure 3. circARNT2 Knockdown Inhibited the Growth of HCC *In Vivo*

(A) The tumor volumes in nude mice injected with sh-circARNT2-transfected Hep3B-R cells were smaller than in the control nude mice; (B) Tendencies in tumor weight were consistent with those in tumor volume; (C) The percentage of Ki67-positive cells in xenografts; All tests were at least performed three times. Data were expressed as mean \pm SD. ** $p < 0.01$.

(WT)-circARNT2 or mutant (MUT)-circARNT2 luciferase reporter plasmids. Then the effect of miR-155-5p on WT-circARNT2 or MUT-circARNT2 luciferase reporter systems was determined. The results showed that miR-155-5p mimic considerably reduced the luciferase activity of the WT-circARNT2 luciferase reporter vector compared with negative control, while miR-155-5p mimic did not pose any impact on the luciferase activity of MUT-circARNT2-transfected Hep3B-R cells ($p < 0.01$, Figure 5C). In a further RIP experiment, circARNT2 and miR-155-5p simultaneously existed in the production precipitated by anti-AGO2 ($p < 0.01$, Figure 5D), suggesting that miR-155-5p is circARNT2-targeting miRNA. Furthermore, silencing of circARNT2 did not affect the expression of miR-155-5p, and transfection of miR-155-5p mimics did not affect the expression of circARNT2 (Figures 5E and 5F), which indicated circARNT2 functions as a miRNA sponge without affecting the expression of sponged miRNAs.

miR-155-5p Suppressed Cisplatin-Resistant HCC Tissues Resistance of HCC Cells

The qRT-PCR analysis indicated that there was a decreasing trend in miR-155-5p levels from normal liver tissues to cisplatin-sensitive HCC tissues and then to cisplatin-resistant HCC tissues, and the differences among the three groups were significant ($p < 0.01$; Figure 6A). We also confirmed that the expression of miR-155-5p was obviously decreased in cisplatin-resistant cells than that in cisplatin-sensitive cells, indicating the opposite result to circARNT2 expression ($p < 0.01$; Figure 6B). To gain insight into whether circARNT2 affected cisplatin resistance of HCC cells via modulation of miR-155-5p, we further performed rescue assays to confirm how miR-155-5p modulated cisplatin resistance. We transfected miR-155-5p mimics or inhibitors into HCC cells and the proliferation curves were performed. Our results showed that Hep3B cells transfected with miR-155-5p inhibitors grew at a dramatically higher rate as compared with controls (Figure 6C; $p < 0.01$), whereas miR-155-5p mimics markedly inhibits the cell growth in Hep3B-R cells when compared with cells transfected with miR-NC (Figure 6D; $p < 0.01$). Moreover, cell proliferation assay proved that downregulation of circARNT2 markedly inhibits the cell growth of Hep3B-R cells, whereas sh-cir-

carNT2#3-induced decrease of cell growth was partially restored by miR-155-5p inhibition (Figure 6E; $p < 0.01$). Furthermore, flow cytometry analysis indicated that circARNT2 knockdown dramatically aggravated cisplatin-induced apoptosis of Hep3B-R cells, however, sh-circARNT2#3-triggered apoptosis was attenuated after cotransfected with miR-155-5p inhibitor (Figure 6F; $p < 0.01$). Together, these data hinted that inhibition of miR-155-5p could significantly reversed circARNT2-mediated cisplatin resistance in HCC cells.

miR-155-5p Inhibits PDK1 and Promotes Autophagy

We sought to explore potential target genes of miR-155-5p. Bioinformatics analysis by using the TargetScan and Findtar algorithm predicted one putative and highly conserved miR-155-5p binding site within the 3' UTR of PDK1 (Figure 7A). Then, we focused on the transcriptional regulation of PDK1 expression by miR-155-5p. We constructed a luciferase reporter gene plasmid containing PDK1 WT 3' UTR and its MUT 3' UTR (Figure 7A). The dual luciferase reporter gene assay showed that the fluorescence enzyme activity was significantly decreased after co-transfection with the PDK1 WT 3' UTR construct and miR-155-5p mimics. In contrast, the fluorescence enzyme activity was nearly unchanged after co-transfection with PDK1 MUT 3' UTR construct and miR-155-5p mimics (Figure 7B). To determine the expression levels of PDK1 in HCC, we investigated the PDK1 expression in the HCC tissues by qRT-PCR. The results showed that PDK1 expression was significantly upregulated in HCC specimens compare with that in the adjacent normal tissues ($p < 0.01$; Figure 7C). To further confirm the effects of circARNT2 on PDK1 expression, we transfected HCC cells with the circARNT2 siRNA and detected the PDK1 mRNA levels by qRT-PCR. The results showed that knockdown of circARNT2 expression significantly reduced the PDK1 mRNA levels in SR-HepG2 cells (Figure 7D). Moreover, inhibition of circARNT2 mediated decrease of PDK1 mRNA expression was significantly recuperated following miR-155-5p inhibitors (Figure 7D).

Previous studies have shown that PDK1 is a critical checkpoint for autophagy dysfunction. To determine the role of miR-155-5p in autophagy, we transfected miR-155-5p mimics into Hep3B-R cells and found that the expression levels P62, a marker of autophagy, was significantly reduced in miR-155-5p-overexpressing cells compared to the

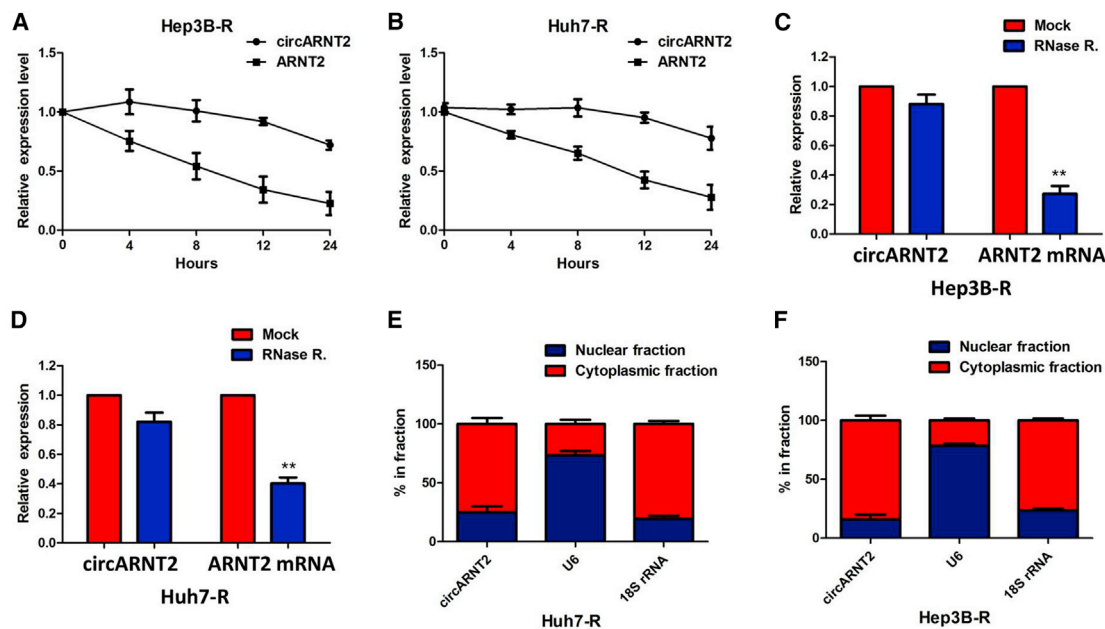


Figure 4. Confirmation of the Circular Structure and Subcellular Localization of circARNT2

(A) qRT-PCR for the abundance of circARNT2 and ARNT2 in Hep3B-R cells treated with Actinomycin D at the indicated time point. (B) qRT-PCR for the abundance of circARNT2 and ARNT2 in Huh7-R cells treated with Actinomycin D at the indicated time point. (C) qRT-PCR for the expression of circARNT2 and ARNT2 mRNA in Hep3B-R cells treated with or without RNase R. (D) qRT-PCR for the expression of circARNT2 and ARNT2 mRNA in Huh7-R cells treated with or without RNase R. (E) Levels of circARNT2 in the nuclear and cytoplasmic fractions of Hep3B-R cells. (F) Levels of circARNT2 in the nuclear and cytoplasmic fractions of Huh7-R cells. Data are listed as means \pm SD of at least three independent experiments. ** $p < 0.01$.

corresponding control cells (Figure 7E). Taken together, the results indicate that autophagy activity could be enhanced with upregulation of miR-155-5p expression. Taken together, our results indicate that circARNT2 positively regulated PDK1 expression by interacting with miR-155-5p, and this is then followed by the inhibition of autophagy.

DISCUSSION

In this study, we explored the effect of circARNT2 on the chemosensitivity of HCC and demonstrate the regulatory mechanism of miR-155-5p/PDK1 signaling pathway. We first discovered that circARNT2 is frequently upregulated in HCC, and its expression significantly correlated with poor clinicopathologic characteristics. Second, our data showed that the high expression of circARNT2 correlated with poor patient prognosis, indicating its applicability as a promising prognostic biomarker in HCC. Third, we demonstrated that the inhibition of circARNT2 reversed the cisplatin resistance of HCC cells and thus inhibited the progression of HCC. Fourth, we revealed that circARNT2 acts as a ceRNA and regulates PDK1-induced autophagy by competing for miR-155-5p. These results suggested that circARNT2 may have the potential to regulate the cisplatin resistance of HCC, in turn promoting the progression of HCC.

In the last decade, improved drug therapy agents have significantly prolonged the survival of HCC patients with advanced diseases.¹⁸ Cisplatin, the first-generation of the platinum chemotherapeutic drugs, can inhibit DNA replication and transcription by forming crosslinks

between DNA double strands and exhibits broad-spectrum antitumor activity. Cisplatin is one of the most commonly used chemotherapeutic agents to treat advanced HCC. However, the acquisition of multi-drug resistance (MDR) to cisplatin is still a major obstacle for HCC patients to obtain a satisfactory curative effect.¹⁹ The role of circRNAs and the underlying mechanisms in HCC has been reported before.²⁰ However, more specific mechanisms of circRNAs in drug resistance of HCC need to be further teased out. Using a circRNA microarray assay, we analyzed aberrantly expressed circRNAs between cisplatin-resistant HCC tissues and cisplatin-sensitive HCC tissues. Results showed that 538 were significantly upregulated and 430 were significantly downregulated in cisplatin-resistant HCC tissues compared with cisplatin-sensitive HCC tissues. Then, we demonstrated that circARNT2 was upregulated in HCC tissues and associated with cisplatin resistance in HCC. To further validate whether circARNT2 functionally required for cisplatin resistance, we performed loss-of-function studies by knockdown circARNT2 in cisplatin-resistant HCC cell lines (Hep3B-R and Huh7-R). Meanwhile, we overexpressed circARNT2 in Hep3B and Huh7 cells. Loss-of-function experiments revealed that knockdown of circARNT2 inhibited the cisplatin-induced cell apoptosis and cell mobility of cisplatin-resistant cells. Gain-of-function experiments revealed that ectopic expression of circARNT2 promoted proliferation and promoted apoptosis of cisplatin sensitive cells, compared with negative control-transfected cells. In addition, xenograft experiments revealed that circARNT2 knockdown inhibited the growth of HCC *in vivo*.

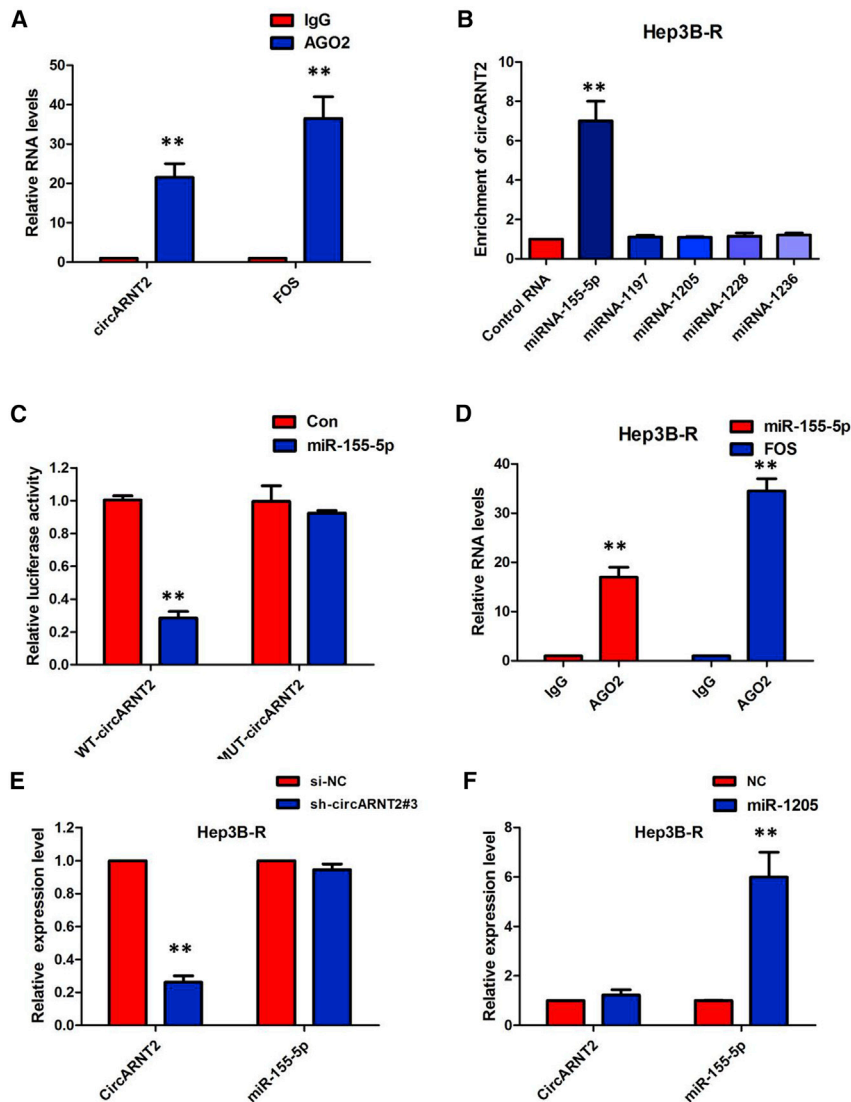


Figure 5. circARNT2 Functioned as a Molecular Sponge of miR-155-5p in HCC Cells

(A) Endogenous circARNT2 was efficiently pulled down by anti-Ago2. (B) miRNA pull-down assay showed that circARNT2 was only efficiently enriched by miR-155-5p. (C) The luciferase reporter systems showed that miR-155-5p mimic considerably reduced the luciferase activity of the WT-circARNT2 luciferase reporter vector compared with negative control, while miR-155-5p mimic did not pose any impact on the luciferase activity of MUT-circARNT2-transfected cells. (D) circARNT2 and miR-155-5p simultaneously existed in the production precipitated by anti-Ago2. (E) Silencing of circARNT2 did not affect the expression of miR-155-5p. (F) Transfection of miR-155-5p mimics did not affect the expression of circARNT2. All tests were at least performed three times. Data were expressed as mean \pm SD. ** $p < 0.01$.

and binds to circARNT2 without promoting the degradation of circARNT2.

In this study, we identified circARNT2 as a new interactive molecule of miRNA-155-5p, also confirmed that PDK1 was a new downstream target of miRNA-155-5p. PDK1 is now widely studied in malignant tumors because PDK1 can serve as an important junction point for multiple cell signaling pathways.²³ The results of qRT-PCR showed that PDK1 expression in HCC specimens was significantly upregulated compare with that in the adjacent normal tissues. circARNT2 could control the PDK1 level by provoking miRNA-155-5p. Previous studies have shown that PDK1 is a critical checkpoint for autophagy dysfunction.²⁴ Autophagy is an important metabolic process for maintaining cell homeostasis. Autophagy reduces protein synthesis and increases protein degradation, thereby inhibiting the proliferation of primary cancer cells and tumor growth.²⁵ We found that the expression of miR-155-5p contrasted with the activity of autophagy marker protein (P62), indicating that upregulation of miR-155-5p induces autophagy in HCC cells.

In conclusion, our study revealed that circARNT2 is frequently activated in cisplatin-resistant HCC tissues and cell lines and associated with a poor survival outcome. These results indicate that circARNT2 functions as an oncogene by sponging miR-155-5p, leading to PDK1 upregulation, and finally sensitizes HCC cells to cisplatin. Therefore, our findings provide significant evidence to further elucidate the therapeutic use of circRNA in HCC.

MATERIALS AND METHODS

Clinical Specimens

A total of 82 pairs of HCC and tumor-adjacent tissues were collected from patients who underwent hepatectomy at the Affiliated Hospital

circRNAs may act as transcription regulators or as sponges for small RNA regulators, which compete for microRNA (miRNA) activity in the process of regulating cell proliferation.²¹ Most circRNAs have miRNA-binding sites that can be used as miRNA sponges to inhibit the regulation of miRNAs on downstream target genes by a large number of miRNAs in cancers.²² Herein, circARNT2 has been shown to target miRNA-155-5p using bioinformatics tools. Intriguingly, the ectopic expression of miRNA-155-5p reduced the luciferase activity of the WT-circARNT2 reporter. However, there was no significant difference in circARNT2 expression upon forced miRNA-155-5p expression. Furthermore, endogenous circARNT2 and miRNA-155-5p were pulled down by a special AGO2 antibody. Ultimately, we found that circARNT2 enhances the cisplatin resistance, mainly through interaction with miRNA-155-5p, and miRNA-155-5p mimics reversed circARNT2-mediated cisplatin resistance effects. Taken together, all of the data suggest that miRNA-155-5p recognizes

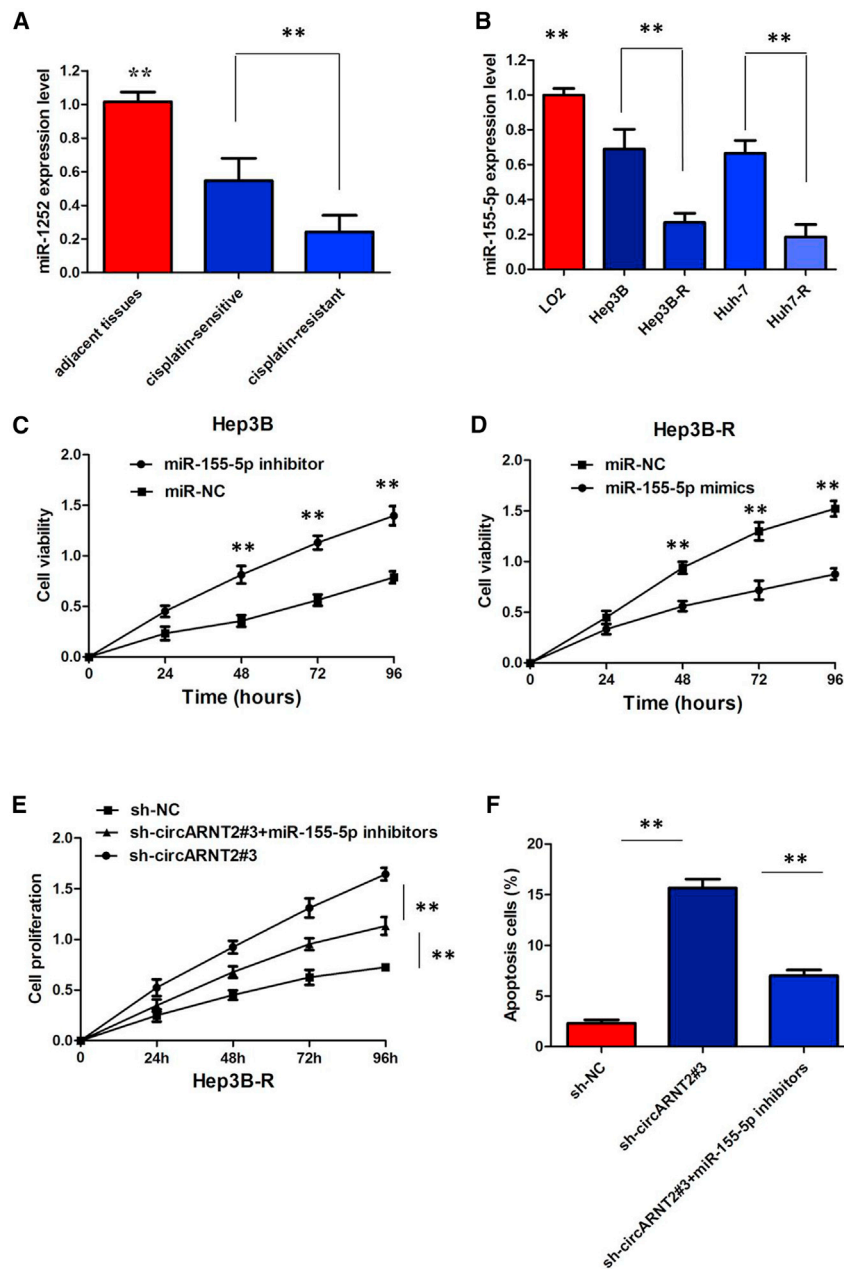


Figure 6. miR-155-5p Suppressed Cisplatin-Resistant HCC Tissues Resistance of HCC Cells

(A) The level of miR-155-5p was significantly decreased in cisplatin-resistant HCC tissues. (B) The level of miR-155-5p was significantly decreased in cisplatin-resistant cells than that in cisplatin sensitive cells. (C) Hep3B cells transfected with miR-155-5p inhibitors grew at a dramatically higher rate as compared with controls. (D) miR-155-5p mimics markedly inhibits the cell growth in Hep3B-R cells when compared with cells transfected with miR-NC (E) Down-regulation of circARNT2-induced decrease of cell growth was partially restored by miR-155-5p inhibition. (F) Down-regulation of circARNT2-triggered apoptosis was attenuated after cotransfection with miR-155-5p inhibitor. All tests were at least performed three times. Data were expressed as mean \pm SD. ** $p < 0.01$.

and RPMI-1640 (GIBCO, Carlsbad, CA) together with 10% fetal bovine serum (GIBCO) at 37°C in an atmosphere containing 5% CO₂. The cisplatin-resistant Hep3B (Hep3B-R) and Huh7 (Huh7-R) cells were prepared according to the method previously described.¹⁸

circRNA Microarray Analysis

Total RNA was extracted from patients with cisplatin-resistant or cisplatin-sensitive HCC using the RNeasy Mini Kit (QIAGEN, GmbH, Hilden, Germany) according to the manufacturer's instructions. The adjacent tissues were used as control. Patients with cisplatin-resistant HCC were defined as those with persistent disease more than 2 months, and those with recurrent disease more than 2 months after completion of chemotherapy containing cisplatin. Patients with cisplatin-sensitive HCC were defined as those without local residual lesions or recurrence at 2 months after completion of chemotherapy containing cisplatin. Purified total RNA was quantified using the NanoDrop 2000 spectrophotometer. The total RNA was sent to Aksomics (Shanghai, China) to analyze

circRNA expression profiles. Differentially expressed circRNAs were identified as FC >2 and adjusted $p < 0.05$.

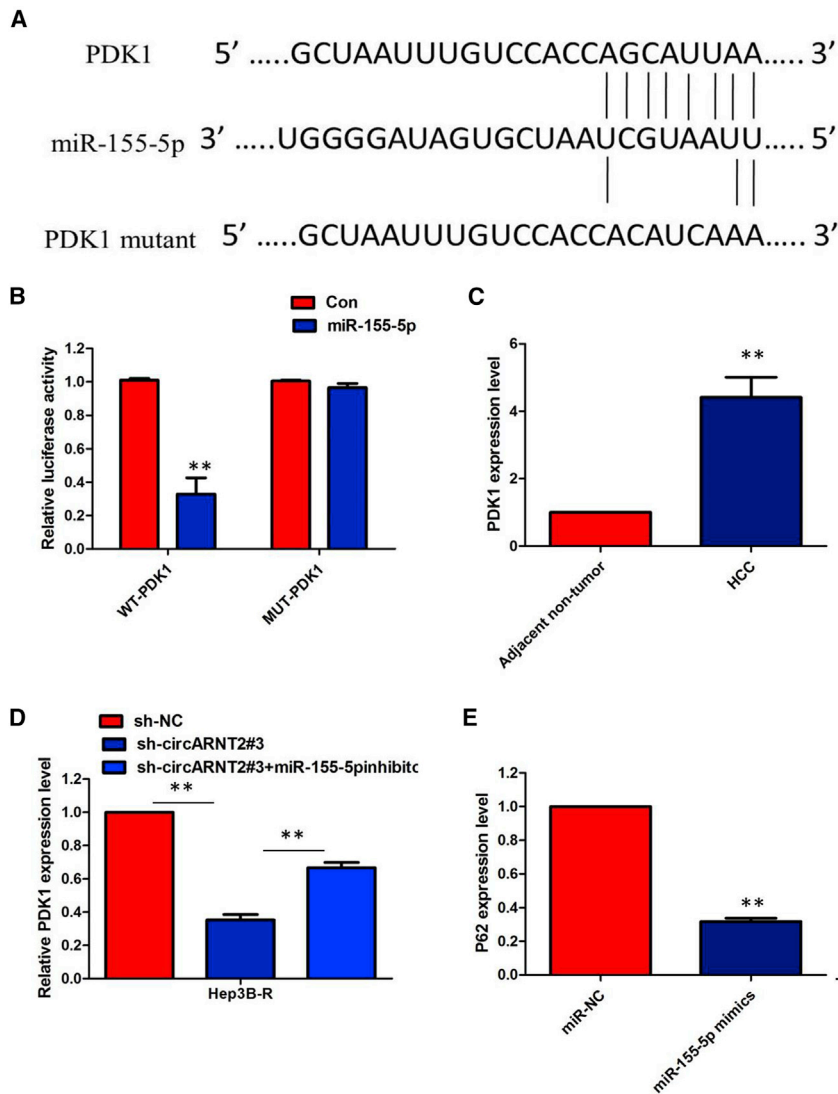
TCGA Dataset Analysis

The data and the corresponding clinical information of patients were collected from The Cancer Genome Atlas (TCGA) database (<http://cancergenome.nih.gov/>). We used the edgeR package of R packages to perform the difference analysis (<http://www.bioconductor.org/packages/release/bioc/html/edgeR.html>) and used the pheatmap package of R packages to perform the cluster analysis (<https://cran.r-project.org/web/packages/pheatmap/index.html>). Sva R package was used to

of Youjiang Medical University for Nationalities. None of HCC patients received any pre-operative treatments, such as RFA, TACE, immunotherapy, and targeted therapy. The tissue samples were confirmed by two histopathologists. All samples were immediately snap-frozen in liquid nitrogen and subsequently stored at -80°C until RNA extraction.

Cell Culture

HCC cell lines Hep3B, Huh-7, and the normal human liver cell line LO2 were purchased from the Chinese Academy of Sciences Cell Bank Type Culture Collection. The cells were cultured with DMEM



remove the batch effect. Genes with adjusted *p* values < 0.05 and absolute FCs > 1.5 were considered differentially expressed genes. Kaplan-Meier survival curves were drawn to analyze the relationships between genes and overall survival in the survival package. The corresponding statistical analysis and graphics were performed in R software (R version 3.3.2).

RNA Isolation and qRT-PCR

RNA was totally extracted from the cells and tissue using the with TRIzol reagent (1 mL; Invitrogen) based on the manufacturer's protocol. The testing for miRNA extraction was mirVana miRNA isolation kit (Ambion, Austin, TX, USA). After isolation, the RNA concentration in the RNA solution was determined using Nano-Drop 1000 spectrophotometer (Thermo Fisher Scientific, Wilmington, DE, USA) and stored at 80°C for further use. Glyceraldehyde-3-phosphate dehydrogenase (GAPDH) was used as an endogenous control.

Figure 7. miR-155-5p Inhibits PDK1 and Promotes Autophagy

(A) Bioinformatics analysis revealed the predicted binding sites between miR-155-5p and PDK1. (B) Luciferase reporter assay demonstrated miR-155-5p mimics significantly decreased the luciferase activity of PDK1-WT in HCC cells. (C) The immunohistochemistry results showed that PDK1 expression in HCC specimens was significantly up-regulated compare with that in the adjacent normal tissues. (D) The western blotting assay showed that inhibition of circARNT2 mediated decrease of PDK1 protein expression was significantly recuperated following miR-155-5p inhibitors. (E) The immunofluorescence assay showed that the expression levels P62 was significantly reduced in miR-155-5p-overexpressing cells compared to the corresponding control cells.

siRNA and Plasmid Construction and Cell Transfection

For transfections, cells at the confluence of 50%–80% were infected with 1×10^6 recombinant lentivirus-transducing units and 6 $\mu\text{g}/\text{mL}$ Polybrene (Sigma, Shanghai, China). Stably transfected cells were selected via treatment with 2 $\mu\text{g}/\text{mL}$ puromycin for 2 weeks. Stably transfected cells were picked via flow cytometry for subsequent assays. Plasmid, lentivirus, miRNA inhibitor, and miRNA mimics used in this study were purchased from GenePharma (Shanghai, China), pHBV1.3 copy was purchased from Miaolingbio (Wuhan, China). Lipofectamine 3000 (Invitrogen, CA, USA) was utilized for transfection.

CCK-8 Assay

After transfection, the cells mixed with 10 mL of CCK-8 solutions per well and incubated for further 1 h at 37°C. The amount of formazan dye generated by cellular dehydrogenase activity was measured for absorbance at 450 nm by a microplate reader (Molecular Devices, Sunnyvale, CA, USA). The optical density values of each well represented the survival/proliferation of HCC cells.

Flow Cytometric Analysis

Transfected cells were harvested after transfection by trypsinization. After the double staining with fluorescein isothiocyanate (FITC)-Annexin V and propidium iodide was done by the FITC Annexin V Apoptosis Detection Kit (BD Biosciences) according to the manufacturer's recommendations, the cells were analyzed with a flow cytometry (FACScan; BD Biosciences) equipped with a Cell Quest software (BD Biosciences). Cells were discriminated into viable cells, dead cells, early apoptotic cells, and apoptotic cells and then the relative ratio of early apoptotic cells were compared with control transfection from each experiment.

Tumor Xenograft in Nude Mice

Animal experiments were approved by the Ethical Committee for Animal Research of the Affiliated Hospital of Youjiang Medical University for Nationalities. Ten nude mice (5 mice per group, male, 2 months old) were purchased from Shanghai Experimental Animal Center (Shanghai, China). Mice were subcutaneously injected into the back with 1×10^6 SR-HepG2 cells transfected with si-circARNT2 or si-NC suspended in 100 μ L Hank's balanced salt solution. The tumor size was measured every 3 days with a caliper, and tumor volume was calculated according to the formula: volume = length \times width²/2. All mice were sacrificed on day 21 after inoculation. The resected tumor masses were harvested for subsequent weight and qRT-PCR analysis.

Actinomycin D and RNase R Treatment

To block transcription, we added 2 mg/mL Actinomycin D or dimethyl sulfoxide (Sigma-Aldrich, St. Louis, MO, USA) as a negative control into the cell culture medium. For RNase R treatment, total RNA (2 μ g) was incubated for 30 min at 37°C with or without 3 U/ μ g of RNase R (Epicenter Technologies, Madison, WI, USA). After treatment with Actinomycin D and RNase R, qRT-PCR was performed to determine the expression levels of circARNT2 and ARNT2 mRNA.

Isolating RNAs from Nucleus and Cytoplasmic Fractions

The nuclear and cytoplasmic fractions were isolated using PARIS Kit (Invitrogen, Carlsbad, CA, USA) following the manufacturer's protocol. Briefly, cells were collected and lysed with cell fractionation buffer, followed by centrifugation to separate the nuclear and cytoplasmic fractions. The supernatant containing the cytoplasmic fraction was collected and transferred to a fresh RNase-free tube. The nuclear pellet was lysed with Cell Disruption Buffer. The cytoplasmic fraction and nuclear lysate were mixed with 2X Lysis/Binding Solution and then added with 100% ethanol. The sample mixture was drawn through a Filter Cartridge, followed by washing with Wash Solution. The RNAs of nuclear and cytoplasmic fractions were eluted with Elution Solution. U6 snRNA and 18S rRNA were employed as positive control for nuclear and cytoplasmic fractions, respectively.

Biotin-Coupled miRNA Capture

Briefly, the 30 end biotinylated miR-RNA mimic or control biotin-RNA (RiboBio) was transfected into SPC-A1 cells at a final concentration of 20 nmol/L for 1 day. The biotin-coupled RNA complex was pulled down by incubating the cell lysate with streptavidin-coated magnetic beads (Ambion, Life Technologies).

Luciferase Reporter Assays

The luciferase reporter assays were carried out with the help of the Dual-Luciferase Reporter Assay System (Promega, Madison, WI, USA). The WT circARNT2 or MUT circARNT2 that had the predicted miR-155-5p binding site was established and integrated into a pmir-GLO dual-luciferase vector to form the pmirGLO-circARNT2-WT or pmirGLO-circARNT2 MUT (circARNT2-MUT) reporter vector. Cotransfection of circARNT2-WT or circARNT2-MUT was carried out with miR-155-5p mimics or negative control

into HCC cells with the use of Lipofectamine 2000. Subsequent to transfection for a period of 48 h, the luciferase activities were measured in accordance with the guidelines of the manufacturer. In the same manner, pmirGLO-PDK1-WT or pmirGLO-PDK1-MUT were constructed, together with cotransfecting with miR-155-5p mimics or negative control into cells. 48 h following the transfection, the relative luciferase activities were detected.

RIP

Magna RIP RNA-Binding Protein Immunoprecipitation Kit (Millipore, Billerica, MA, USA) were used for RIP. Cells were lysed in complete RNA lysis buffer, then cell lysates were incubated with RIP buffer containing magnetic beads conjugated with human anti-AGO2 antibody (Millipore) or negative control mouse immunoglobulin G (IgG; Millipore).

Statistical Analysis

Results are presented expressed as mean \pm SD (standard deviation). Student's t test was performed to measure the difference between two group and differences between more than two groups were assessed using one-way ANOVA. $p < 0.05$ was considered significant.

SUPPLEMENTAL INFORMATION

Supplemental Information can be found online at <https://doi.org/10.1016/j.omtn.2020.08.037>.

AUTHOR CONTRIBUTIONS

Y.L. and Y.Z. performed primers design and experiments. S.Z. and G.L. contributed flow cytometry assay and animal experiments. Y.W. and Q.J. collected and classified the human tissue samples. L.L. contributed to RT-PCR and qRT-PCR. C.L. analyzed the data. Y.L. and Z.W. wrote the paper. All authors read and approved the final manuscript.

CONFLICTS OF INTEREST

The authors declare no competing interests.

ACKNOWLEDGMENTS

This project was funded by National Natural Science Foundation of China 81860320, Guangxi Traditional Chinese Medicine and Ethnic Medicine Self-Funded Research Project gzzc15-76, and Scientific Research and Technology Development Project of Baise City, Guangxi 20120113. We have received consent from individual patients who have participated in this study. The consent forms will be provided upon request.

REFERENCES

- Bray, F., Ferlay, J., Soerjomataram, I., Siegel, R.L., Torre, L.A., and Jemal, A. (2018). Global cancer statistics 2018: GLOBOCAN estimates of incidence and mortality worldwide for 36 cancers in 185 countries. *CA Cancer J. Clin.* 68, 394–424.
- Chan, A.W.H., Zhong, J., Berhane, S., Toyoda, H., Cucchetti, A., Shi, K., Tada, T., et al. (2018). Development of pre and post-operative models to predict early recurrence of hepatocellular carcinoma after surgical resection. *J. Hepatol.* 69, 1284–1293.
- Yang, J.D., and Roberts, L.R. (2010). Hepatocellular carcinoma: A global view. *Nat. Rev. Gastroenterol. Hepatol.* 7, 448–458.

4. El-Serag, H.B., Marrero, J.A., Rudolph, L., and Reddy, K.R. (2008). Diagnosis and treatment of hepatocellular carcinoma. *Gastroenterology* 134, 1752–1763.
5. El-Serag, H.B. (2011). Hepatocellular carcinoma. *N. Engl. J. Med.* 365, 1118–1127.
6. Harlan, L.C., Parsons, H.M., Wiggins, C.L., Stevens, J.L., and Patt, Y.Z. (2015). Treatment of hepatocellular carcinoma in the community: disparities in standard therapy. *Liver Cancer* 4, 70–83.
7. Jeck, W.R., and Sharpless, N.E. (2014). Detecting and characterizing circular RNAs. *Nat. Biotechnol.* 32, 453–461.
8. Li, Z., Ruan, Y., Zhang, H., Shen, Y., Li, T., and Xiao, B. (2019). Tumor-suppressive circular RNAs: Mechanisms underlying their suppression of tumor occurrence and use as therapeutic targets. *Cancer Sci.* 110, 3630–3638.
9. Hansen, T.B., Jensen, T.L., Clausen, B.H., Bramsen, J.B., Finsen, B., Damgaard, C.K., and Kjems, J. (2013). Natural RNA circles function as efficient microRNA sponges. *Nature* 495, 384–388.
10. Li, Y., Zheng, Q., Bao, C., Li, S., Guo, W., Zhao, J., Chen, D., Gu, J., He, X., and Huang, S. (2015). Circular RNA is enriched and stable in exosomes: a promising biomarker for cancer diagnosis. *Cell Res.* 25, 981–984.
11. Zhang, H., Deng, T., Ge, S., Liu, Y., Bai, M., Zhu, K., Fan, Q., Li, J., Ning, T., Tian, F., et al. (2019). Exosome circRNA secreted from adipocytes promotes the growth of hepatocellular carcinoma by targeting deubiquitination-related USP7. *Oncogene* 38, 2844–2859.
12. Yao, T., Chen, Q., Shao, Z., Song, Z., Fu, L., and Xiao, B. (2018). Circular RNA 0068669 as a new biomarker for hepatocellular carcinoma metastasis. *J. Clin. Lab. Anal.* 32, e22572.
13. Huang, X.Y., Huang, Z.L., Huang, J., Xu, B., Huang, X.Y., Xu, Y.H., Zhou, J., and Tang, Z.Y. (2020). Exosomal circRNA-100338 promotes hepatocellular carcinoma metastasis via enhancing invasiveness and angiogenesis. *J. Exp. Clin. Cancer Res.* 39, 20.
14. Fu, L., Wu, S., Yao, T., Chen, Q., Xie, Y., Ying, S., Chen, Z., Xiao, B., and Hu, Y. (2018). Decreased expression of hsa_circ_0003570 in hepatocellular carcinoma and its clinical significance. *J. Clin. Lab. Anal.* 32, 22239.
15. Guarnerio, J., Bezzi, M., Jeong, J.C., Paffenholz, S.V., Berry, K., Naldini, M.M., Lo-Coco, F., Tay, Y., Beck, A.H., and Pandolfi, P.P. (2016). Oncogenic role of fusion-circRNAs derived from Cancer-associated chromosomal translocations. *Cell* 165, 289–302.
16. Zheng, Q., Bao, C., Guo, W., Li, S., Chen, J., Chen, B., Luo, Y., Lyu, D., Li, Y., Shi, G., et al. (2016). Circular RNA profiling reveals an abundant circHIPK3 that regulates cell growth by sponging multiple miRNAs. *Nat. Commun.* 7, 11215.
17. Memczak, S., Jens, M., Elefsinioti, A., Torti, F., Krueger, J., Rybak, A., Maier, L., Mackowiak, S.D., Gregersen, L.H., Munschauer, M., et al. (2013). Circular RNAs are a large class of animal RNAs with regulatory potency. *Nature* 495, 333–338.
18. Shen, Y.C., Lin, Z.Z., Hsu, C.H., Hsu, C., Shao, Y.Y., and Cheng, A.L. (2013). Clinical trials in hepatocellular carcinoma: an update. *Liver Cancer* 2, 345–364.
19. Kalyan, A., Nimeiri, H., and Kulik, L. (2015). Systemic therapy of hepatocellular carcinoma: current and promising. *Clin. Liver Dis.* 19, 421–432.
20. Wang, M., Yu, F., and Li, P. (2018). Circular RNAs: characteristics, function and clinical significance in hepatocellular carcinoma. *Cancers (Basel)* 10, E258.
21. Fu, L., Jiang, Z., Li, T., Hu, Y., and Guo, J. (2018). Circular RNAs in hepatocellular carcinoma: Functions and implications. *Cancer Med.* 7, 3101–3109.
22. Qiu, L.P., Wu, Y.H., Yu, X.F., Tang, Q., Chen, L., and Chen, K.P. (2018). The emerging role of circular RNAs in hepatocellular carcinoma. *J. Cancer* 9, 1548–1559.
23. Gagliardi, P.A., Puliafito, A., and Primo, L. (2017). PDK1: at the crossroad of cancer signaling pathways. *Semin. Cancer Biol.* 48, 30110–30114.
24. Wang, R., Zhang, Q., Peng, X., Zhou, C., Zhong, Y., Chen, X., Qiu, Y., Jin, M., Gong, M., and Kong, D. (2016). Stelletin B induces G1 arrest, apoptosis and autophagy in human non-small cell lung cancer A549 cells via blocking PI3K/Akt/mTOR pathway. *Sci. Rep.* 6, 27071.
25. Kimmelman, A.C. (2011). The dynamic nature of autophagy in cancer. *Genes Dev.* 25, 1999–2010.